

Supplementary Material

Table S1. The mean and range values of the three bioclimate variables for the observed 1976–1985 data and for the 2079–2100 climate scenario data.

| Climatic Variable | Observed | A1b | | | | A2 | | | | |
|-------------------|-----------|---------|-------|--------|---------|---------|-------|--------|---------|--------|
| | 1976–1985 | Average | ECHAM | GFDL | HADGEM1 | Average | ECHAM | GFDL | HADGEM1 | |
| MTWA (°C) | mean | 18.96 | 22.40 | 22.38 | 22.17 | 22.63 | 22.71 | 22.41 | 22.43 | 23.29 |
| | minimum | 4.57 | | 6.90 | 5.50 | 8.50 | | 6.90 | 5.70 | 8.70 |
| | maximum | 27.46 | | 31.50 | 31.80 | 31.30 | | 31.70 | 32.50 | 31.80 |
| PRE (mm) | mean | 55.90 | 52.11 | 54.47 | 50.39 | 51.47 | 50.60 | 53.34 | 48.24 | 50.22 |
| | minimum | 13.22 | | 10.35 | 9.28 | 8.05 | | 9.15 | 9.63 | 7.13 |
| | maximum | 149.37 | | 178.32 | 184.37 | 178.20 | | 172.55 | 179.62 | 174.32 |
| SST (°C) | mean | 10.08 | 13.09 | 13.07 | 12.72 | 13.49 | 13.28 | 13.08 | 12.92 | 13.84 |
| | minimum | 0.30 | | 1.970 | 0.67 | 2.38 | | 1.97 | 0.96 | 2.78 |
| | maximum | 19.00 | | 21.17 | 20.60 | 20.47 | | 21.19 | 20.63 | 21.21 |

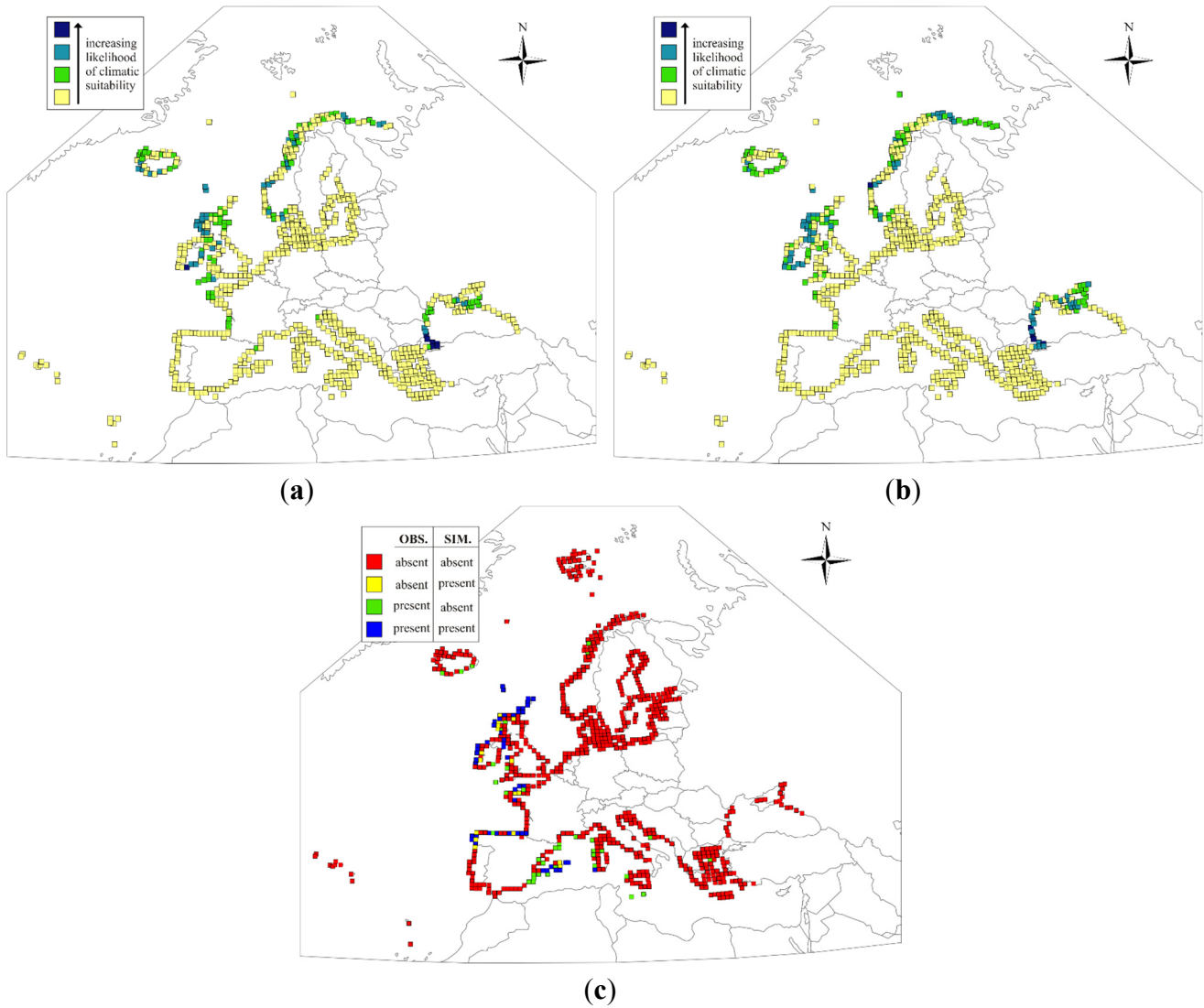


Figure S1. The potential European breeding distribution of European Storm Petrel in 2100 under emissions scenarios A1b (a) and A2 (b) based on climatic suitability predicted for the climatic scenarios derived from three GCMs (yellow—unsuitable under all three GCMs; light green—suitable under one GCM; dark green—suitable under two GCMs; dark blue—suitable under all three GCMs); The observed (OBS) and simulated (SIM) distributions in 1985 are also shown for comparison (c).

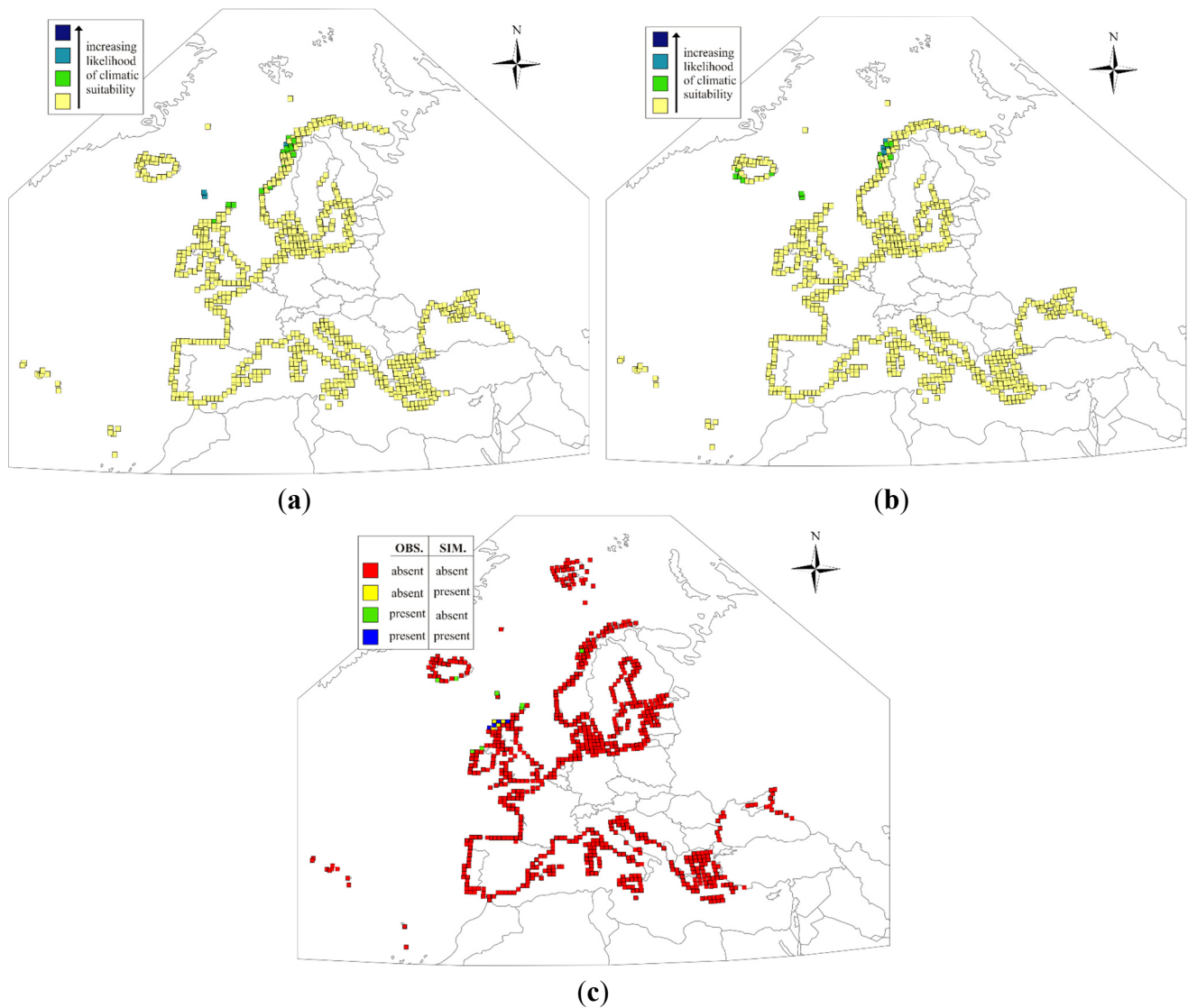


Figure S2. The potential European breeding distribution of the Leach's Storm Petrel in 2100 under emissions scenarios A1b (a) and A2 (b) based on climatic suitability predicted for the climatic scenarios derived from three GCMs (yellow—unsuitable under all three GCMs; light green—suitable under one GCM; dark green—suitable under two GCMs; dark blue—suitable under all three GCMs); The observed (OBS) and simulated (SIM) distributions in 1985 are also shown for comparison (c).

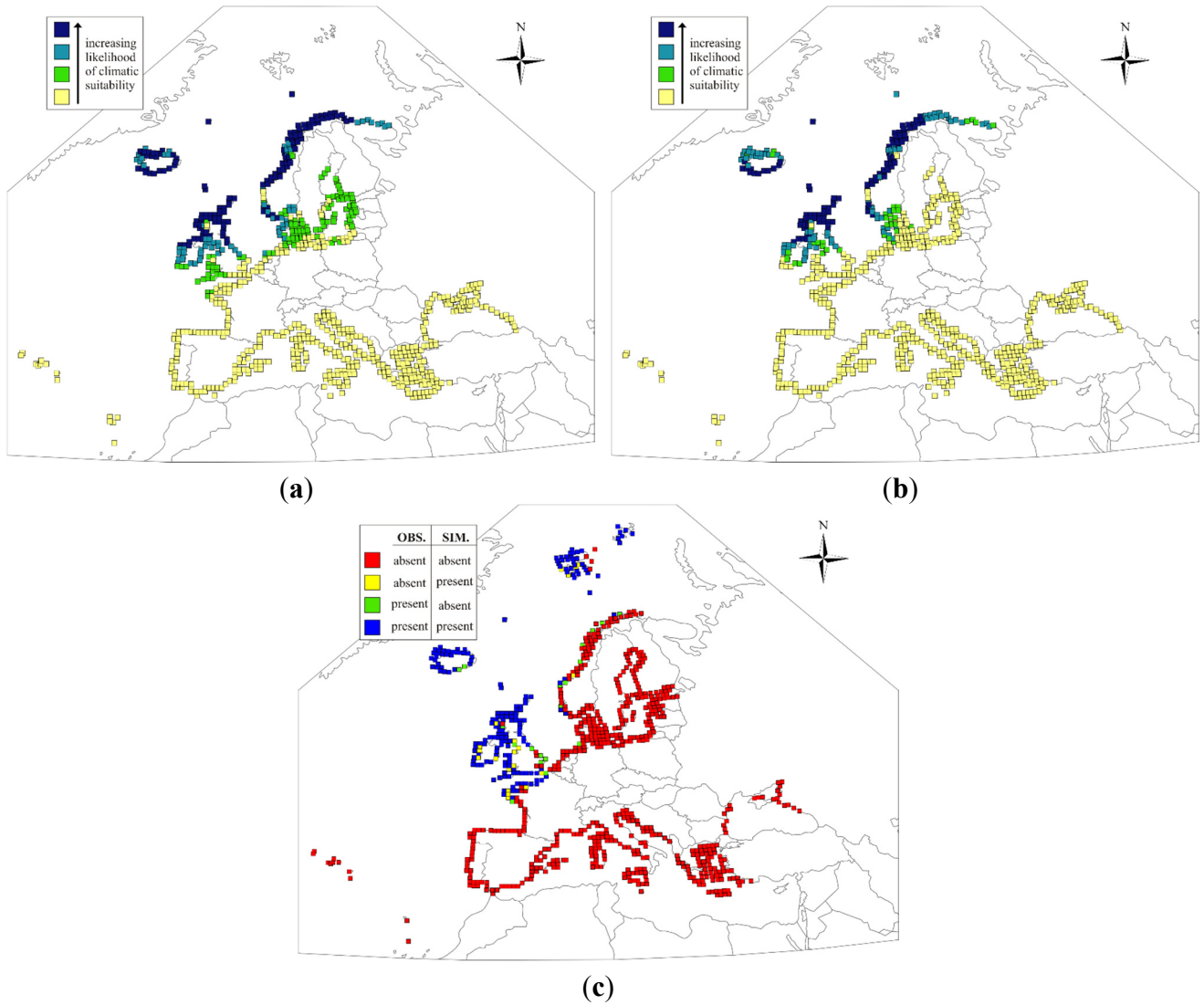


Figure S3. The potential European breeding distribution of the Northern Fulmar in 2100 under emissions scenarios A1b (a) and A2 (b) based on climatic suitability predicted for the climatic scenarios derived from three GCMs (yellow—unsuitable under all three GCMs; light green—suitable under one GCM; dark green—suitable under two GCMs; dark blue—suitable under all three GCMs); The observed (OBS) and simulated (SIM) distributions in 1985 are also shown for comparison (c).

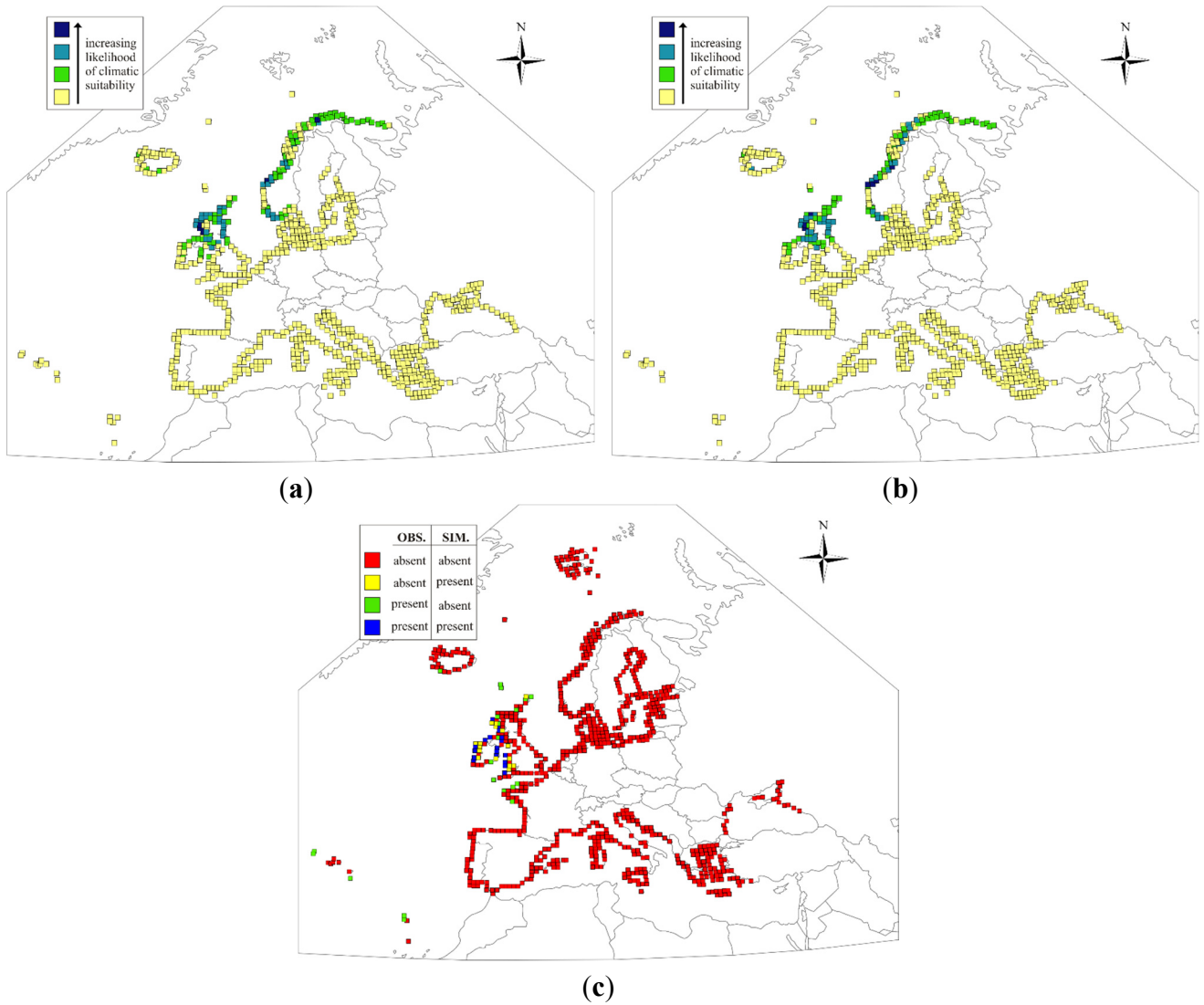


Figure S4. The potential European breeding distribution of the Manx Shearwater in 2100 under emissions scenarios A1b (a) and A2 (b) based on climatic suitability predicted for the climatic scenarios derived from three GCMs (yellow—unsuitable under all three GCMs; light green—suitable under one GCM; dark green—suitable under two GCMs; dark blue—suitable under all three GCMs); The observed (OBS) and simulated (SIM) distributions in 1985 are also shown for comparison (c).

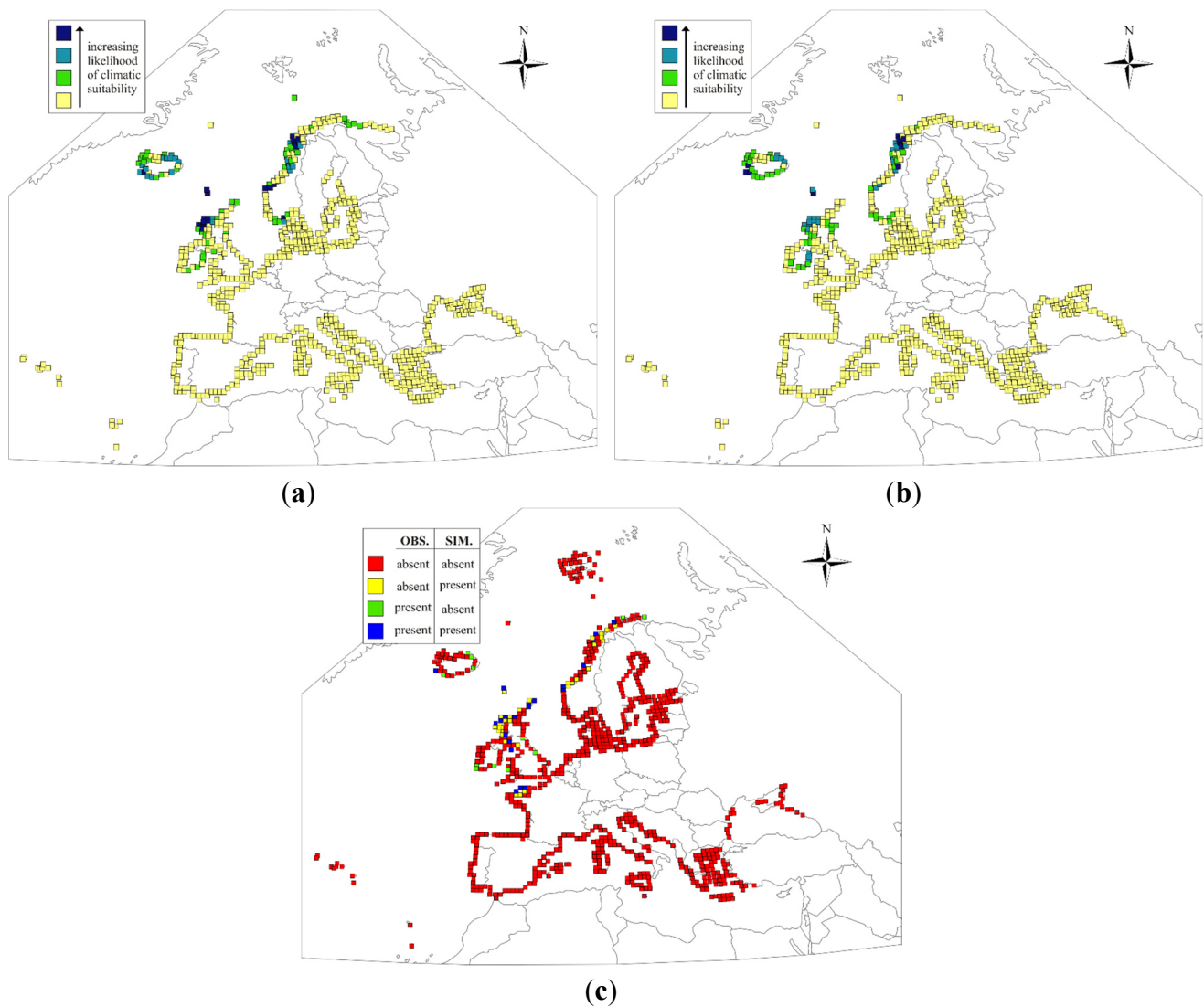


Figure S5. The potential European breeding distribution of the Northern Gannet in 2100 under emissions scenarios A1b (a) and A2 (b) based on climatic suitability predicted for the climatic scenarios derived from three GCMs (yellow—unsuitable under all three GCMs; light green—suitable under one GCM; dark green—suitable under two GCMs; dark blue—suitable under all three GCMs); The observed (OBS) and simulated (SIM) distributions in 1985 are also shown for comparison (c).

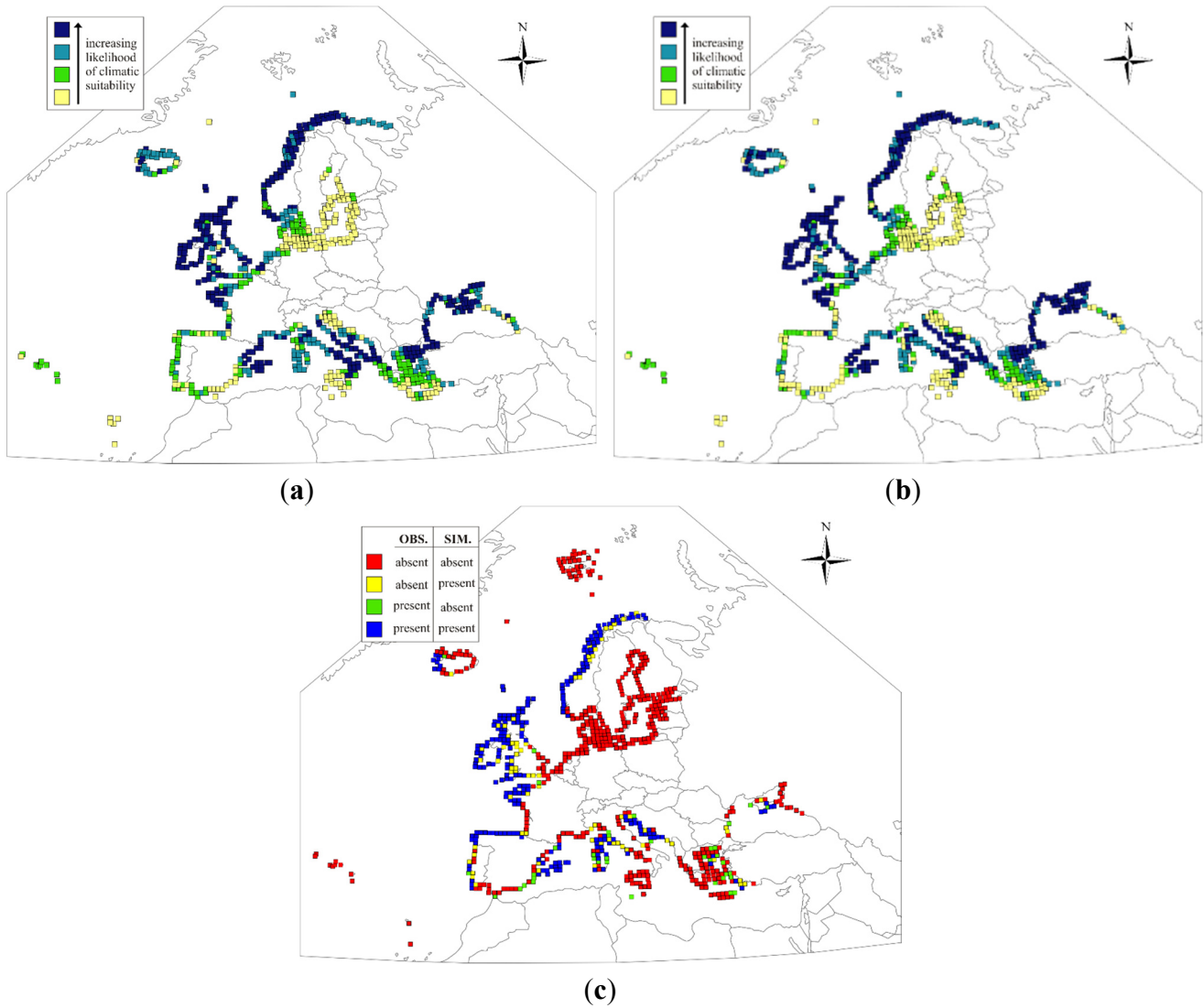


Figure S6. The potential European breeding distribution of the European Shag in 2100 under emissions scenarios A1b (a) and A2 (b) based on climatic suitability predicted for the climatic scenarios derived from three GCMs (yellow—unsuitable under all three GCMs; light green—suitable under one GCM; dark green—suitable under two GCMs; dark blue—suitable under all three GCMs); The observed (OBS) and simulated (SIM) distributions in 1985 are also shown for comparison (c).

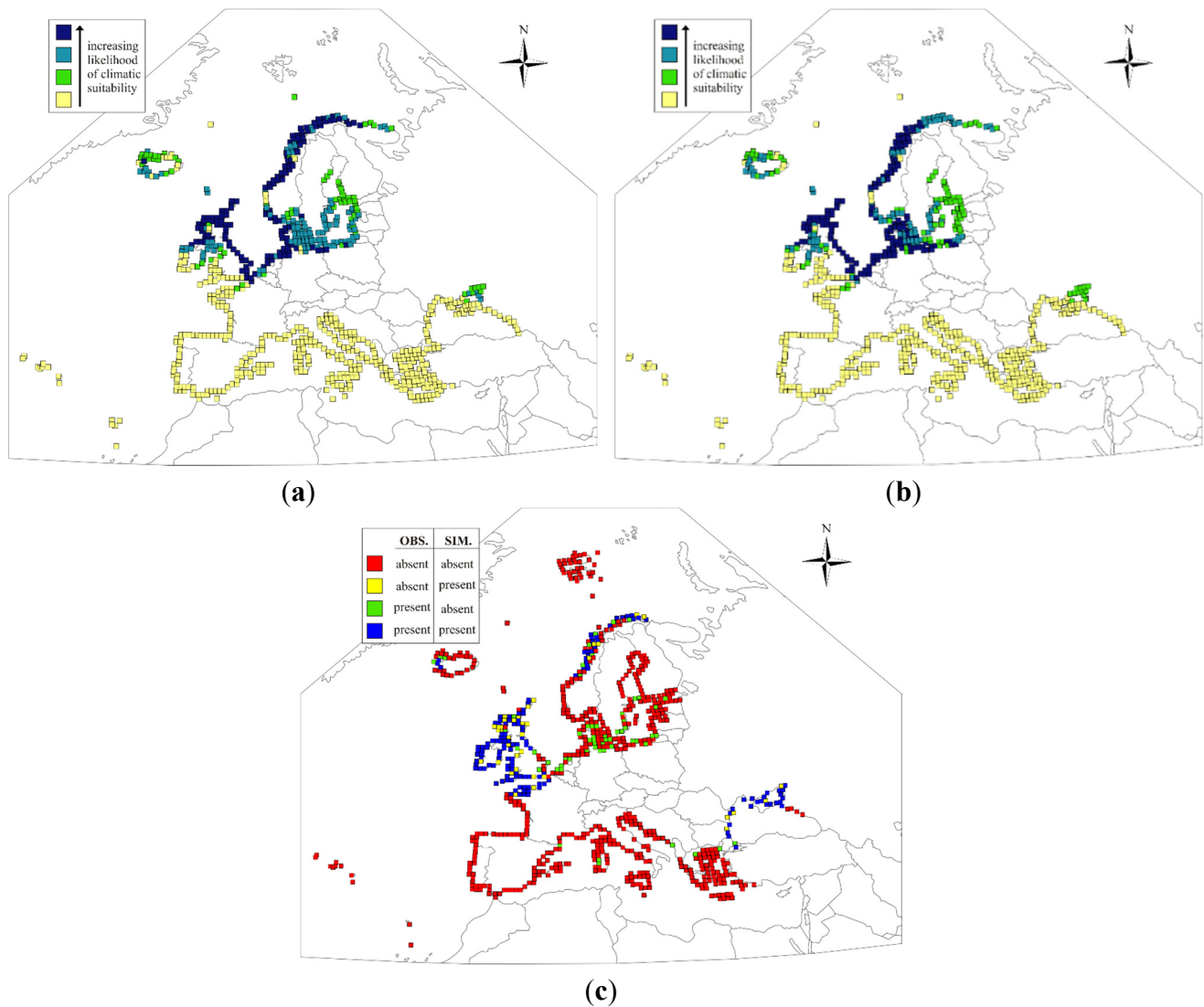


Figure S7. The potential European breeding distribution of the Great Cormorant in 2100 under emissions scenarios A1b (a) and A2 (b) based on climatic suitability predicted for the climatic scenarios derived from three GCMs (yellow—unsuitable under all three GCMs; light green—suitable under one GCM; dark green—suitable under two GCMs; dark blue—suitable under all three GCMs); The observed (OBS) and simulated (SIM) distributions in 1985 are also shown for comparison (c).

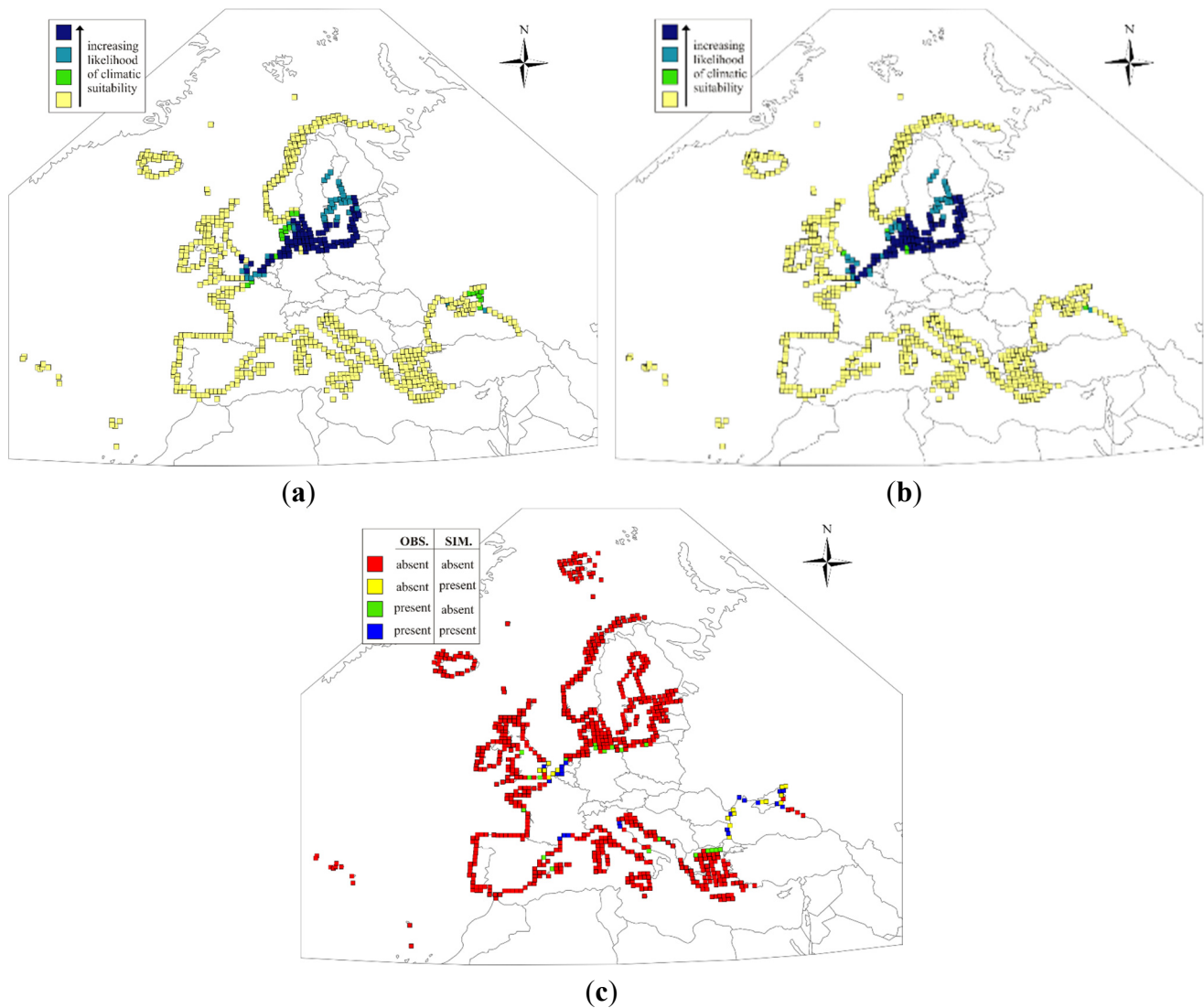


Figure S8. The potential European breeding distribution of the Mediterranean Gull in 2100 under emissions scenarios A1b (a) and A2 (b) based on climatic suitability predicted for the climatic scenarios derived from three GCMs (yellow—unsuitable under all three GCMs; light green—suitable under one GCM; dark green—suitable under two GCMs; dark blue—suitable under all three GCMs); The observed (OBS) and simulated (SIM) distributions in 1985 are also shown for comparison (c).

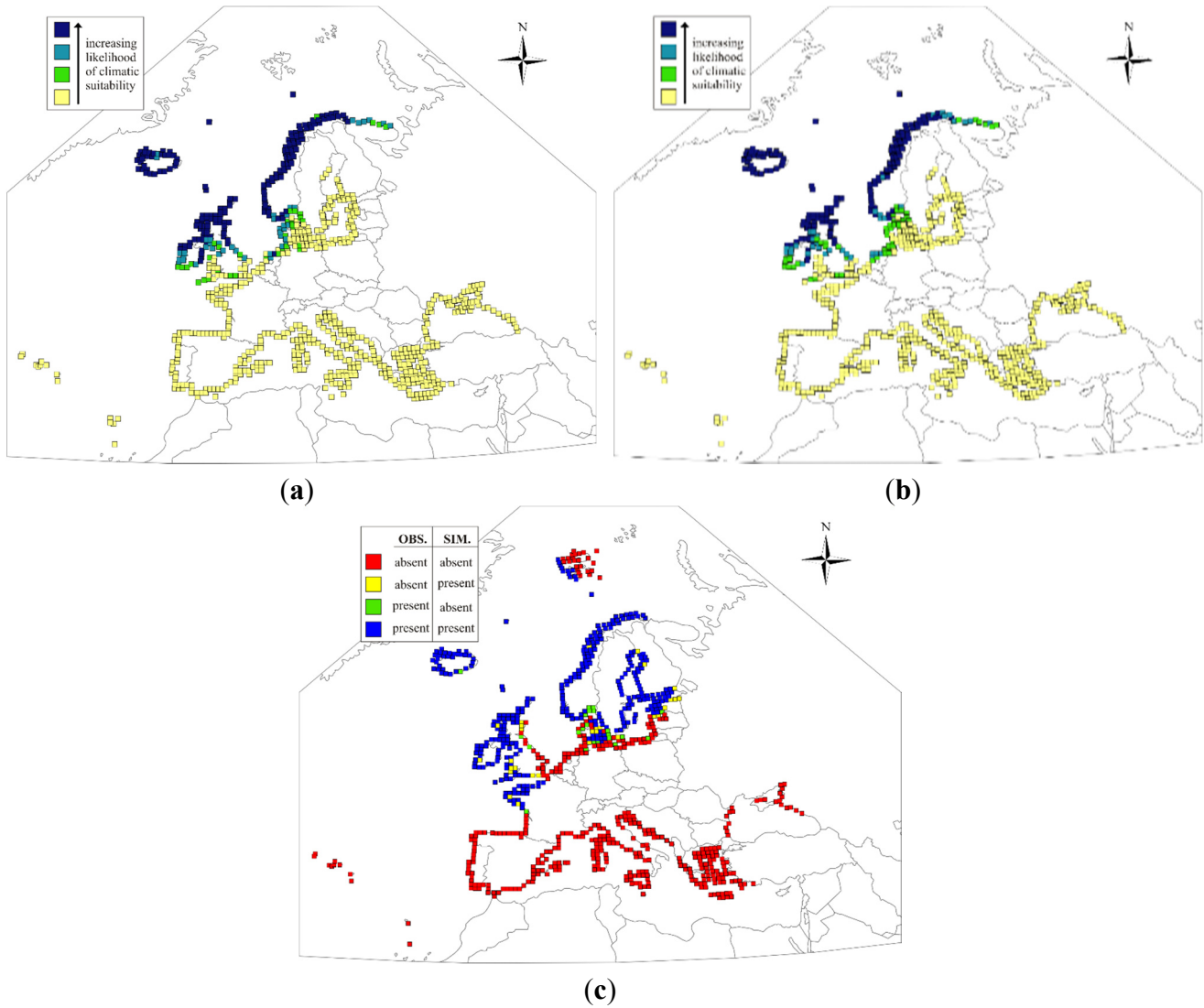


Figure S9. The potential European breeding distribution of the Great Black-backed Gull in 2100 under emissions scenarios A1b (a) and A2 (b) based on climatic suitability predicted for the climatic scenarios derived from three GCMs (yellow—unsuitable under all three GCMs; light green—suitable under one GCM; dark green—suitable under two GCMs; dark blue—suitable under all three GCMs); The observed (OBS) and simulated (SIM) distributions in 1985 are also shown for comparison (c).

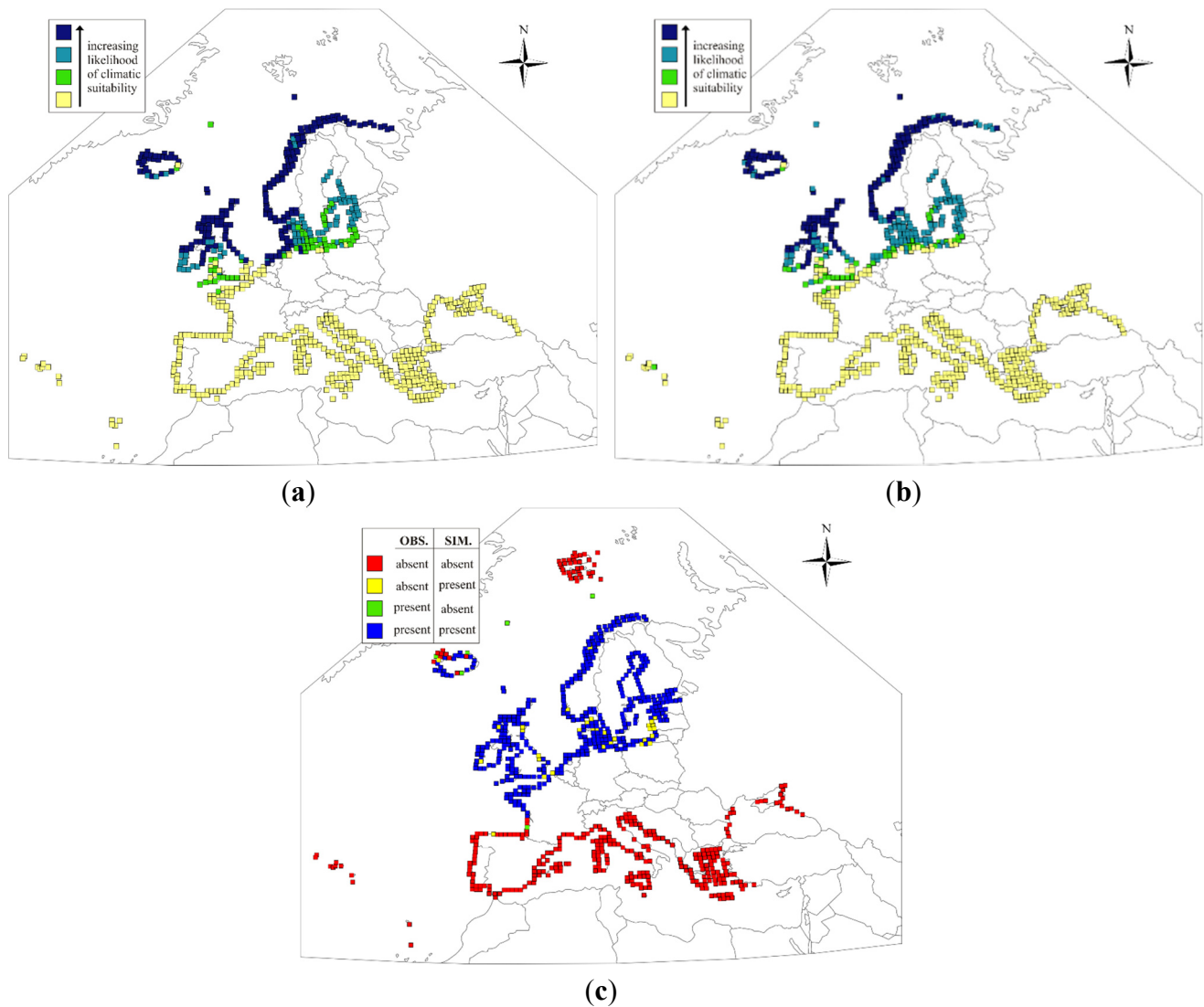


Figure S10. The potential European breeding distribution of the European Herring Gull in 2100 under emissions scenarios A1b (a) and A2 (b) based on climatic suitability predicted for the climatic scenarios derived from three GCMs (yellow—unsuitable under all three GCMs; light green—suitable under one GCM; dark green—suitable under two GCMs; dark blue—suitable under all three GCMs); The observed (OBS) and simulated (SIM) distributions in 1985 are also shown for comparison (c).

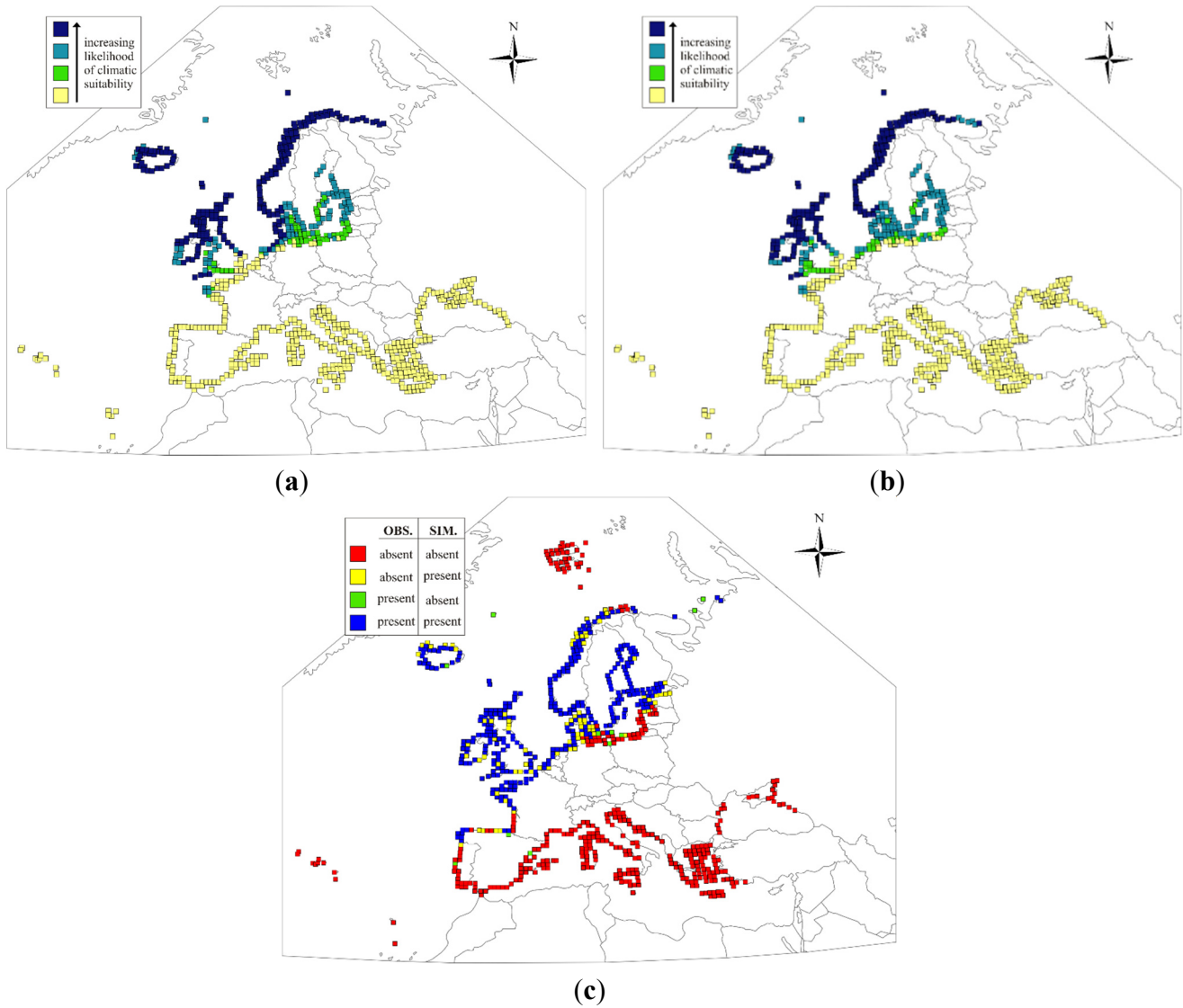


Figure S11. The potential European breeding distribution of the Lesser Black-backed Gull in 2100 under emissions scenarios A1b (a) and A2 (b) based on climatic suitability predicted for the climatic scenarios derived from three GCMs (yellow—unsuitable under all three GCMs; light green—suitable under one GCM; dark green—suitable under two GCMs; dark blue—suitable under all three GCMs); The observed (OBS) and simulated (SIM) distributions in 1985 are also shown for comparison (c).

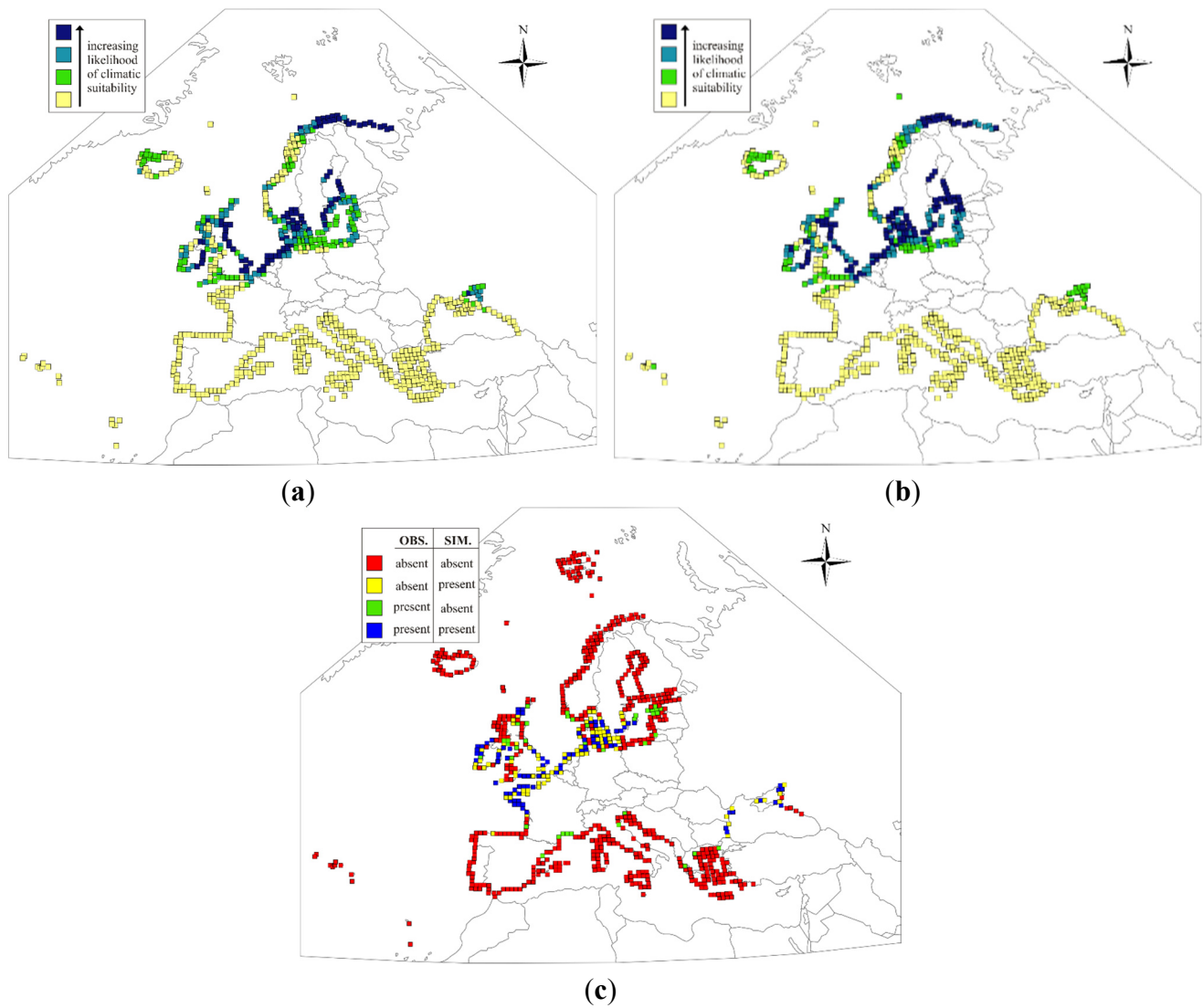


Figure S12. The potential European breeding distribution of the Sandwich Tern in 2100 under emissions scenarios A1b (a) and A2 (b) based on climatic suitability predicted for the climatic scenarios derived from three GCMs (yellow—unsuitable under all three GCMs; light green—suitable under one GCM; dark green—suitable under two GCMs; dark blue—suitable under all three GCMs); The observed (OBS) and simulated (SIM) distributions in 1985 are also shown for comparison (c).

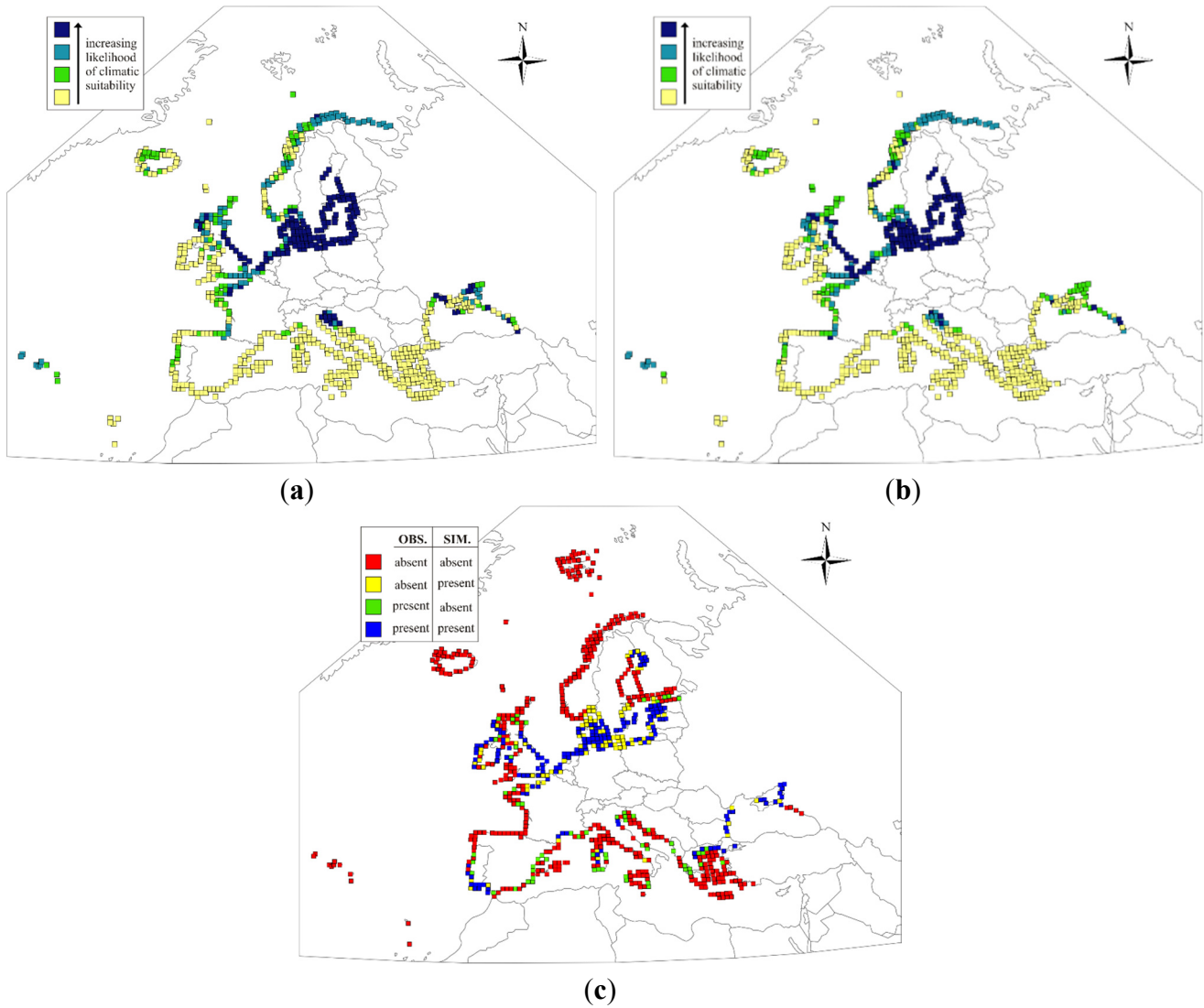


Figure S13. The potential European breeding distribution of the Little Tern in 2100 under emissions scenarios A1b (a) and A2 (b) based on climatic suitability predicted for the climatic scenarios derived from three GCMs (yellow—unsuitable under all three GCMs; light green—suitable under one GCM; dark green—suitable under two GCMs; dark blue—suitable under all three GCMs); The observed (OBS) and simulated (SIM) distributions in 1985 are also shown for comparison (c).

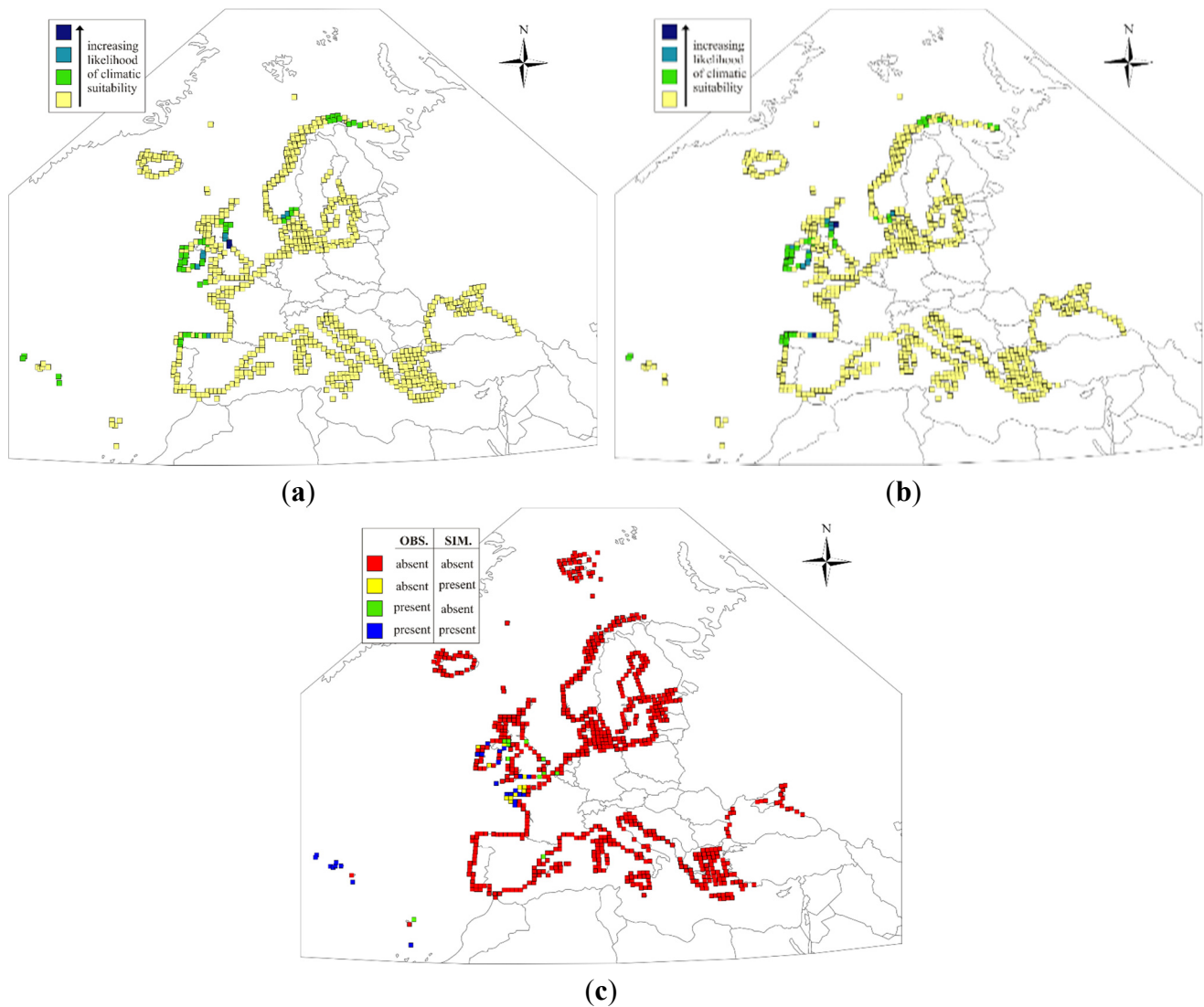


Figure S14. The potential European breeding distribution of the Roseate Tern in 2100 under emissions scenarios A1b (a) and A2 (b) based on climatic suitability predicted for the climatic scenarios derived from three GCMs (yellow—unsuitable under all three GCMs; light green—suitable under one GCM; dark green—suitable under two GCMs; dark blue—suitable under all three GCMs); The observed (OBS) and simulated (SIM) distributions in 1985 are also shown for comparison (c).

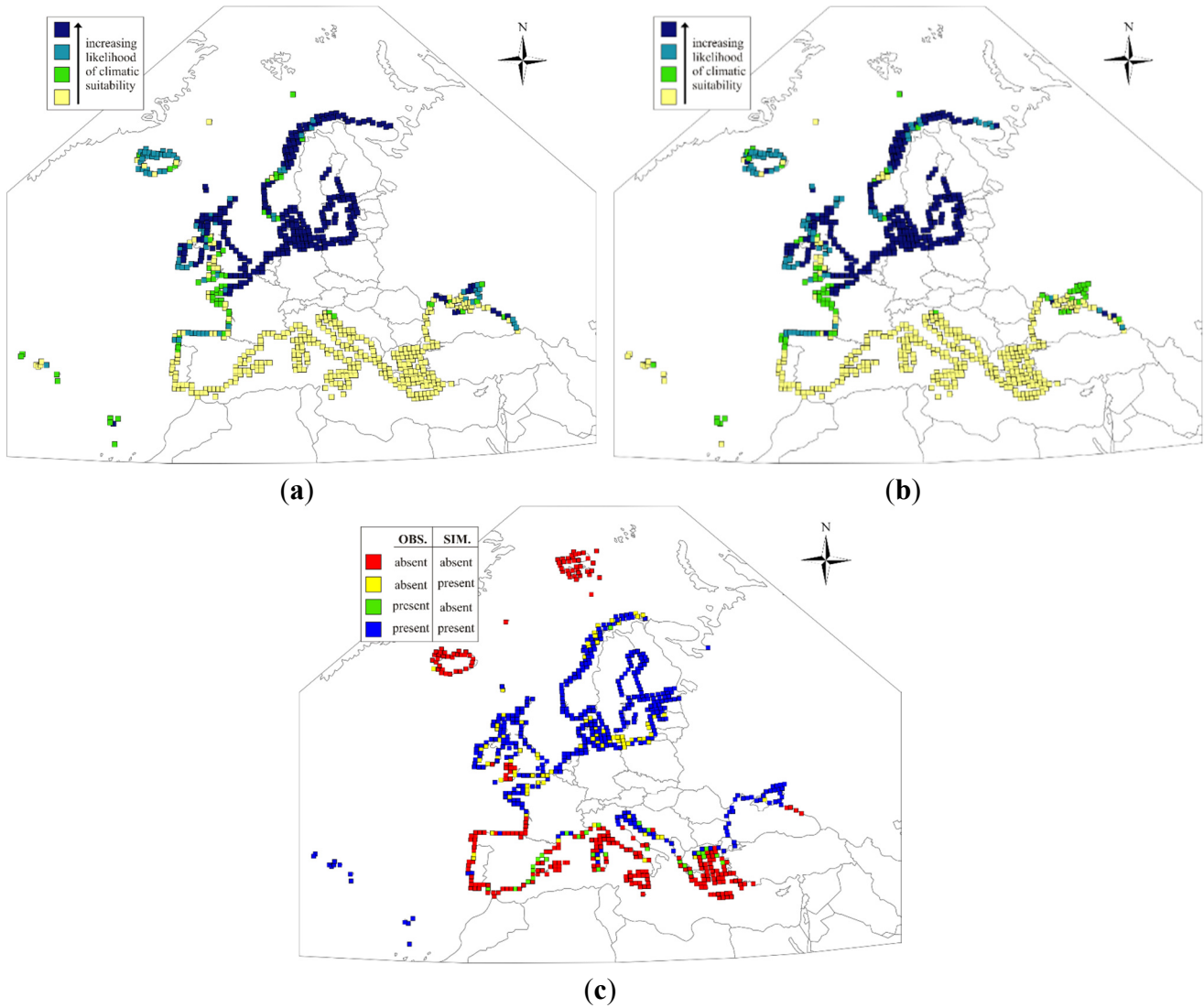


Figure S15. The potential European breeding distribution of the Common Tern in 2100 under emissions scenarios A1b (a) and A2 (b) based on climatic suitability predicted for the climatic scenarios derived from three GCMs (yellow—unsuitable under all three GCMs; light green—suitable under one GCM; dark green—suitable under two GCMs; dark blue—suitable under all three GCMs); The observed (OBS) and simulated (SIM) distributions in 1985 are also shown for comparison (c).

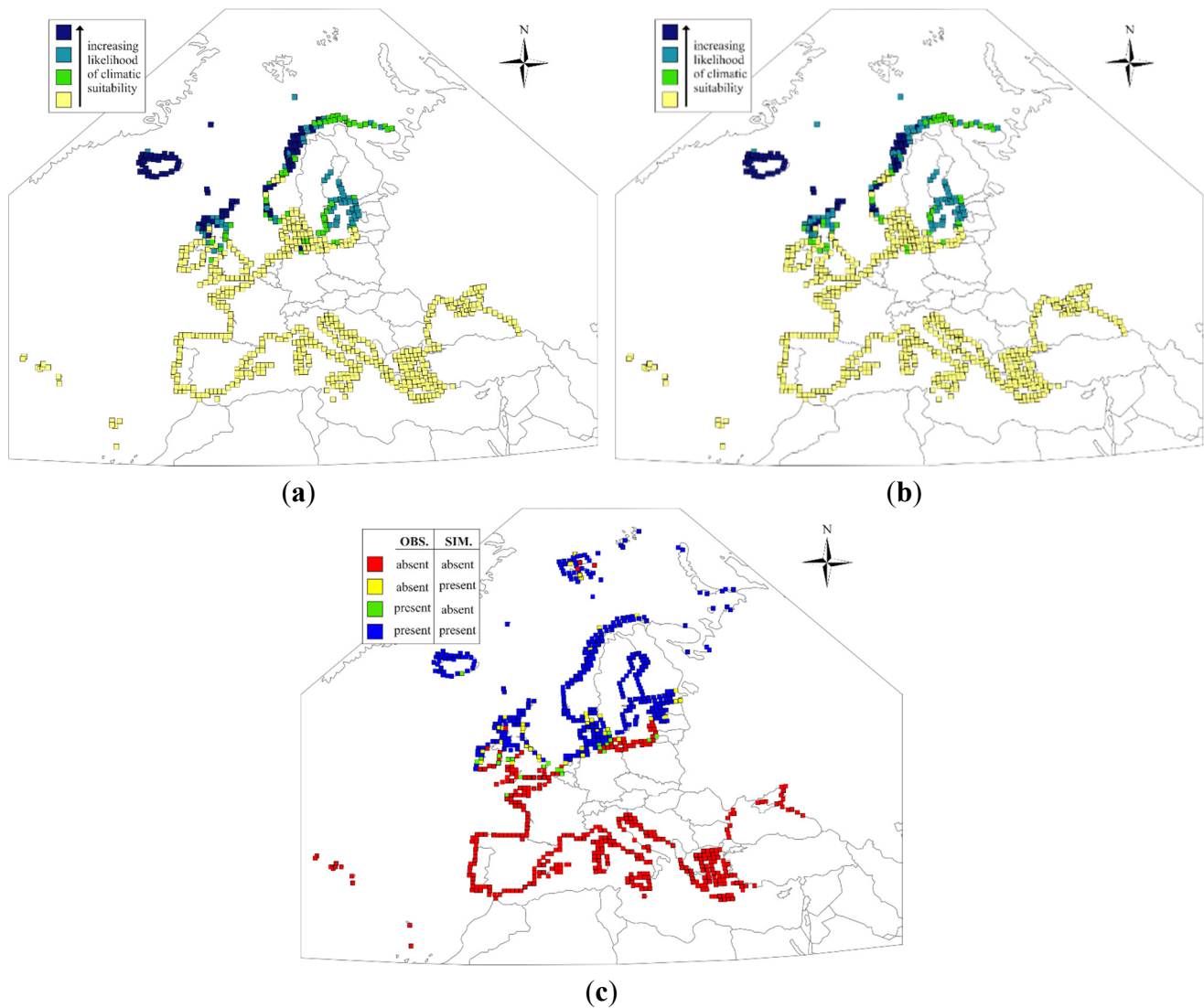


Figure S16. The potential European breeding distribution of the Arctic Tern in 2100 under emissions scenarios A1b (a) and A2 (b) based on climatic suitability predicted for the climatic scenarios derived from three GCMs (yellow—unsuitable under all three GCMs; light green—suitable under one GCM; dark green—suitable under two GCMs; dark blue—suitable under all three GCMs); The observed (OBS) and simulated (SIM) distributions in 1985 are also shown for comparison (c).

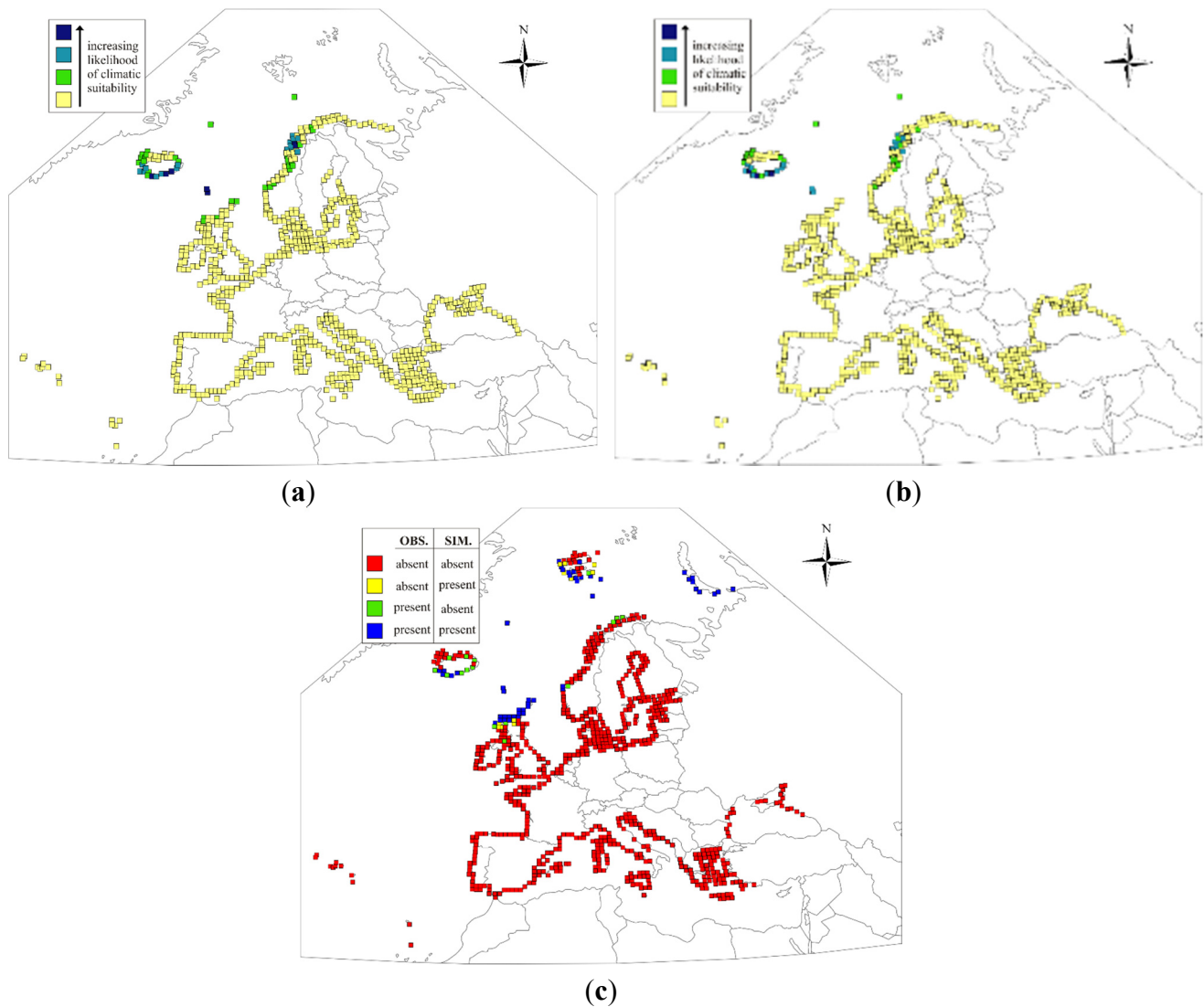


Figure S17. The potential European breeding distribution of the Great Skua in 2100 under emissions scenarios A1b (a) and A2 (b) based on climatic suitability predicted for the climatic scenarios derived from three GCMs (yellow—unsuitable under all three GCMs; light green—suitable under one GCM; dark green—suitable under two GCMs; dark blue—suitable under all three GCMs); The observed (OBS) and simulated (SIM) distributions in 1985 are also shown for comparison (c).

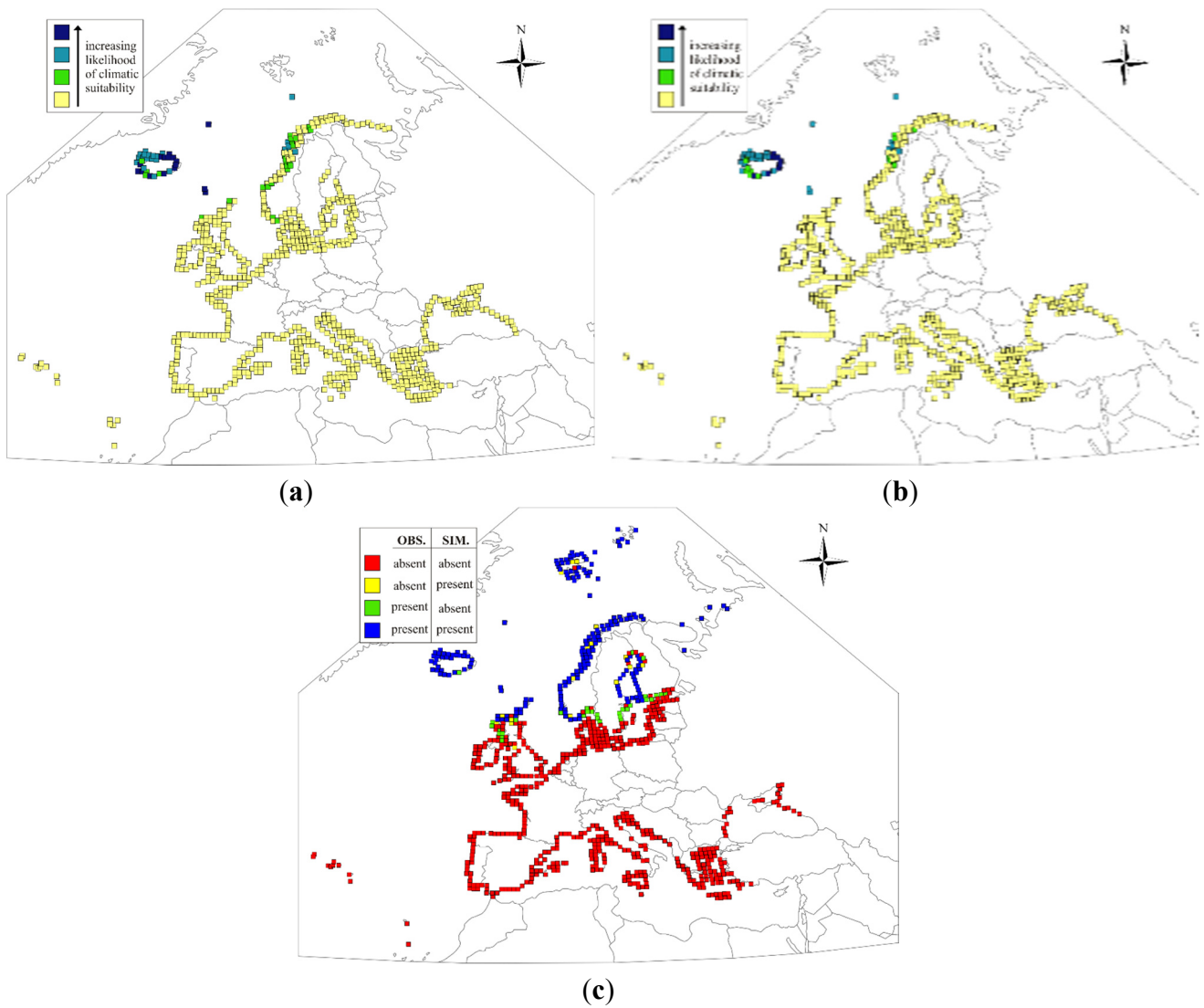


Figure S18. The potential European breeding distribution of the Parasitic Jaeger in 2100 under emissions scenarios A1b (a) and A2 (b) based on climatic suitability predicted for the climatic scenarios derived from three GCMs (yellow—unsuitable under all three GCMs; light green—suitable under one GCM; dark green—suitable under two GCMs; dark blue—suitable under all three GCMs); The observed (OBS) and simulated (SIM) distributions in 1985 are also shown for comparison (c).

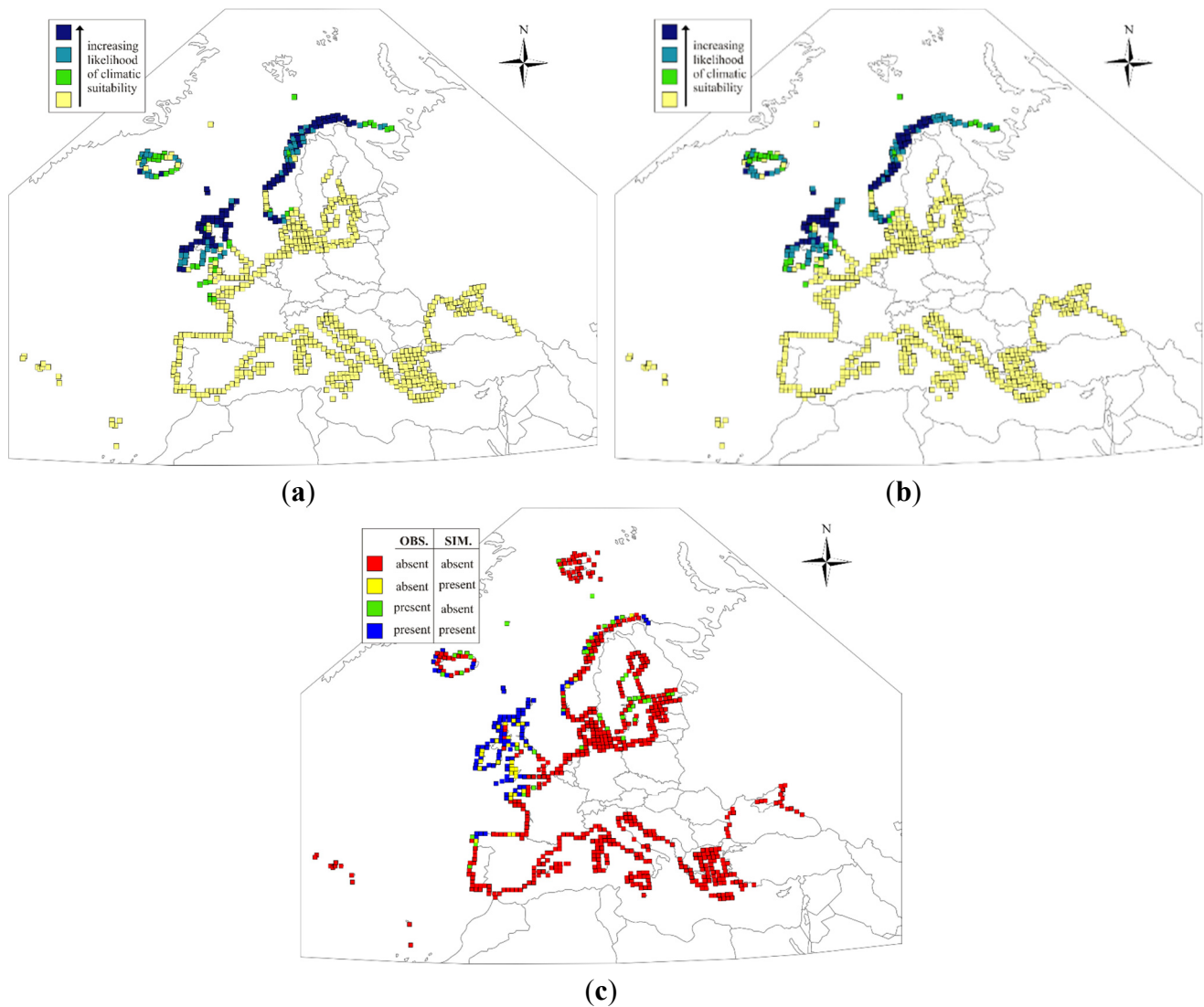


Figure S19. The potential European breeding distribution of the Common Murre in 2100 under emissions scenarios A1b (a) and A2 (b) based on climatic suitability predicted for the climatic scenarios derived from three GCMs (yellow—unsuitable under all three GCMs; light green—suitable under one GCM; dark green—suitable under two GCMs; dark blue—suitable under all three GCMs); The observed (OBS) and simulated (SIM) distributions in 1985 are also shown for comparison (c).

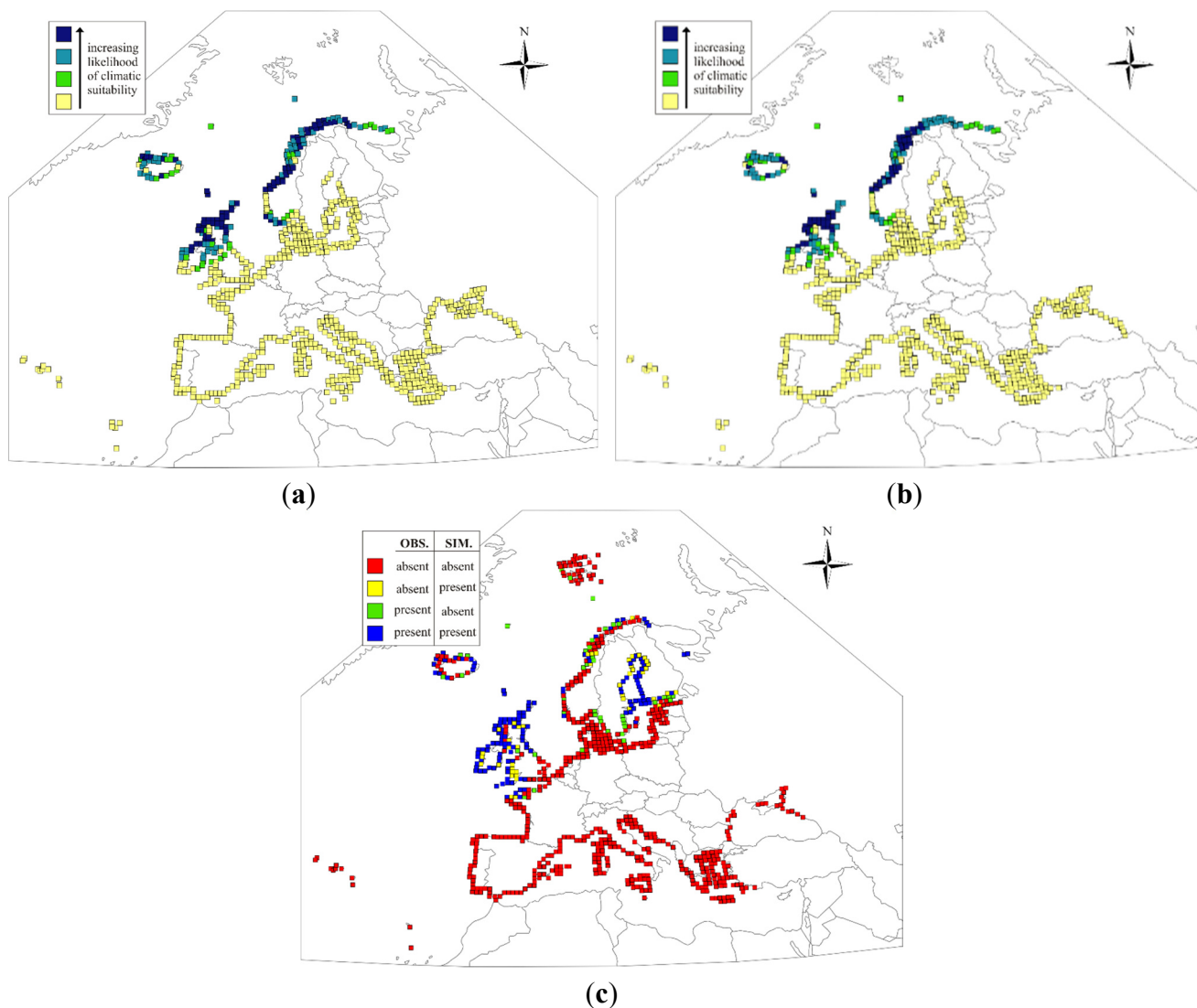


Figure S20. The potential European breeding distribution of the Razorbill in 2100 under emissions scenarios A1b (a) and A2 (b) based on climatic suitability predicted for the climatic scenarios derived from three GCMs (yellow—unsuitable under all three GCMs; light green—suitable under one GCM; dark green—suitable under two GCMs; dark blue—suitable under all three GCMs); The observed (OBS) and simulated (SIM) distributions in 1985 are also shown for comparison (c).

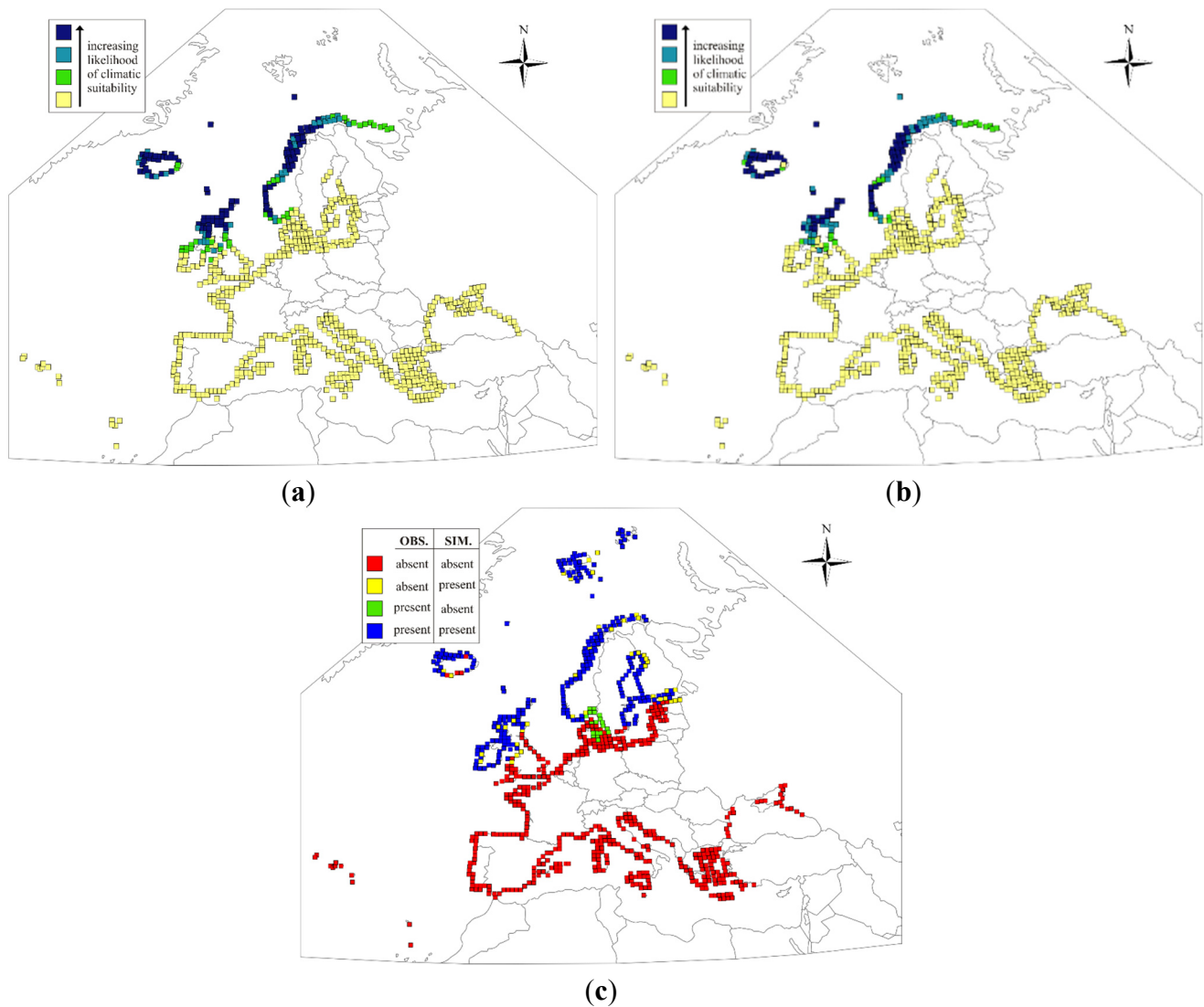


Figure S21. The potential European breeding distribution of the Black Guillemot in 2100 under emissions scenarios A1b (a) and A2 (b) based on climatic suitability predicted for the climatic scenarios derived from three GCMs (yellow—unsuitable under all three GCMs; light green—suitable under one GCM; dark green—suitable under two GCMs; dark blue—suitable under all three GCMs); The observed (OBS) and simulated (SIM) distributions in 1985 are also shown for comparison (c).

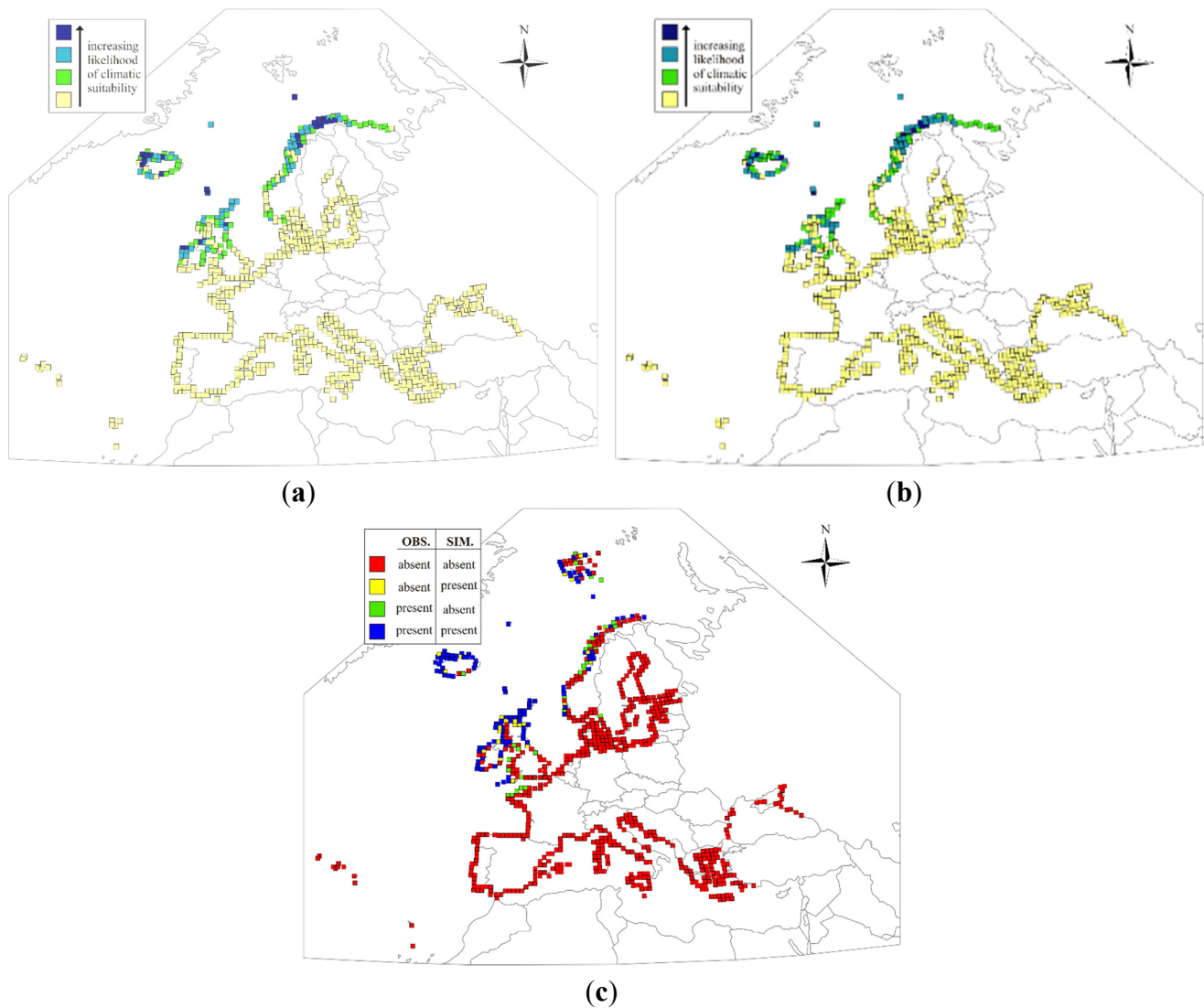


Figure S22. The potential European breeding distribution of the Atlantic Puffin in 2100 under emissions scenarios A1b (a) and A2 (b) based on climatic suitability predicted for the climatic scenarios derived from three GCMs (yellow—unsuitable under all three GCMs; light green—suitable under one GCM; dark green—suitable under two GCMs; dark blue—suitable under all three GCMs); The observed (OBS) and simulated (SIM) distributions in 1985 are also shown for comparison (c).